VO_2 films with strong semiconductor to metal phase transition prepared by the precursor oxidation process

M. Gurvitch
Department of Physics and Astronomy, SUNY at Stony Brook, Stony Brook, New York 11794 and NY State Center for Advanced Sensor Technology, SUNY at Stony Brook, Stony Brook, New York 11794

S. Luryi[a)]
Department of Electrical and Computer Engineering, SUNY at Stony Brook, Stony Brook, New York 11794 and NY State Center for Advanced Sensor Technology, SUNY at Stony Brook, Stony Brook, New York 11794

A. Polyakov and A. Shabalov
NY State Center for Advanced Sensor Technology, SUNY at Stony Brook, Stony Brook, New York 11794

M. Dudley, G. Wang, and S. Ge
Department of Material Science, SUNY at Stony Brook, Stony Brook, New York 11794

V. Yakovlev
Department of Physics, University of Wisconsin—Milwaukee, P.O. Box 413, Milwaukee, Wisconsin 53201

(Received 29 May 2007; accepted 15 June 2007; published online 3 August 2007)

We describe a relatively simple, reliable, and reproducible preparation technique, the precursor oxidation process, for making VO_2 films with strong semiconductor-to-metal phase transition. Sputter-deposited metal precursor V films were oxidized *in situ* in the deposition chamber for 2.5–7 h at 370–415 °C in 0.2 Torr O_2 to form 22–220 nm VO_2. The strength [resistivity ratio, $RR=\rho_S/\rho_M$] and sharpness (hysteresis width ΔT_C) of T-dependent semiconductor-to-metal hysteretic phase transition in VO_2 were our most immediate and relevant quality indicators. In 200-nm-range films, the process was optimized to yield $RR=(1-2)\times 10^3$, $\Delta T_C \sim 11$ °C and absolute resistivity in a semiconducting phase $\rho_S=0.4\pm 0.2$ Ω m, close to resistivity in bulk single crystals of VO_2. Films were characterized by scanning electron microscopy, atomic force microscopy, grazing-incidence x-ray diffraction, and Raman spectroscopy, and found to be polycrystalline single-phase VO_2. We also measured optical reflectivity $R_T(\lambda)$ from 200 to 1100 nm, and $R_\lambda(T)$ from 20 to 100 °C. $R_T(\lambda)$ measured in thin-film interference structures allowed us to calculate the index of refraction in the two phases, which agrees well with the published data and, together with structural measurements, confirms that our films are essentially pure VO_2. The limited study of these films in terms of stability, aging, lithographic processing, and thermal cycling shows that they can be used in applications. © *2007 American Institute of Physics*.
[DOI: 10.1063/1.2764245]

I. INTRODUCTION AND BACKGROUND

The remarkable first order semiconductor-to-metal phase transition (SMPT) in VO_2 at or around 68 °C has been studied for almost half-century.[1,2] In addition to fundamental interest in the nature of this phase transition, a variety of applications were proposed and, for the most part, experimentally tested, as described in papers and patents too numerous to be listed here: resistive switching elements, thermal relays, optical storage devices, holographic recording media, variable reflectivity mirrors, light modulators, energy-efficient windows, flat panel displays, and more.

At Stony Brook we are interested in several electrical and optical applications of VO_2 which utilize the SMPT,[3,4] as well as in the physics of its hysteretic transition. Thus we developed and optimized a relatively simple and reliable method of thin-film VO_2 preparation, which we call the precursor oxidation process (POP). We characterized our films morphologically [optical microscope, scanning electron microscope (SEM), atomic force microscope (AFM)], structurally [grazing-incidence x-ray diffraction (GIXRD) measurements in High-Intensity National Synchrotron Light Source at BNL, Raman spectroscopy], electrically (resistivity ρ vs T from 25 to 100 °C), and optically [$R_T(\lambda)$, reflectivity at fixed T vs λ from 200 to 1100 nm, and $R_\lambda(T)$, reflectivity at fixed λ vs T from 25 to 100 °C]. The rationale for studying resistivity and optical reflectivity in the context of this paper stems from their usefulness as characterization techniques as well as from our desire to produce films that exhibit a well-pronounced SMPT and are well suited for applications. Reflectivity measurements in thin-film interference structures further allowed us to calculate the refractive index in the semiconducting (S) and metallic (M) phases, which turned

[a)]Electronic mail: serge.luryi@stonybrook.edu

 © 2007 American Institute of Physics

out to be in fine agreement with the published values of refractive index in VO_2 obtained by ellipsometry, thus reconfirming that our films are essentially of VO_2 phase.

We have demonstrated that POP is a reproducible and reliable method of film preparation. Our films are stable against aging, multiple cycling through the transition, and with respect to film processing (photolithography, including resist baking and lift-off, and liquid-acid etching). Furthermore, in order to be useful in applications, it is important for the resistivity and optical reflectivity to have stable, time-independent values at a fixed bias temperature within the hysteresis loop. We have established such stability in our films within the limits of our measuring precision.

In order to place our preparation method, POP, in perspective, we shall briefly review VO_2 thin-film preparation techniques. We did not attempt to give a comprehensive list of references on VO_2 preparation techniques. We cite specific references to emphasize features that distinguish POP from other methods, especially results obtained for ultrathin films and including, whenever possible, the temperature coefficient of resistivity (TCR).

Due to the small compositional differences between numerous phases of vanadium oxides,[2,7] VO_2 preparation requires a stringent process control that provides a desired oxygen stoichiometry and correct crystalline structure. In search of such a process, VO_2 films were produced by a number of methods, including dc and rf reactive magnetron sputtering,[5–10,46] reactive ion-beam sputtering,[11–14] reactive evaporation,[15,16] chemical vapor deposition (CVD),[17–19] pulsed laser deposition (PLD),[20–23,49] electrochemical (anodic) oxidation,[24] and sol-gel process.[25]

The resultant film structures varied. Depending on the crystallographic relationship between the growing VO_2 and the substrate, as well as on other factors, such as the growth temperature, some of these methods produced amorphous or quasiamorphous, others polycrystalline, and still others oriented epitaxial films. The best films [i.e., films with the highest ratio of resistivities in S and M phases, $RR=\rho_S/\rho_M$ and the smallest hysteresis width ΔT_C] were prepared at 500–600 °C on single-crystalline substrates having epitaxial relationship to the growing VO_2. Yet nonepitaxial, polycrystalline VO_2 films also exhibit the phase transition, although with a smaller RR and wider hysteresis. Surprisingly, the transition persists even in nearly amorphous ("x-ray amorphous") films, such as in films obtained by anodic oxidation of vanadium. The transition in VO_2 is apparently quite tolerant to the loss of long-range order. Of course, it ultimately depends on the intended application whether a film with a given transition is satisfactory or not, and often, when epitaxial growth is impossible or impractical, one has to compromise.

Study of the literature shows that more often than not, the initially obtained VO_x films were subsequently annealed in various atmospheres (in air, in O_2, in N_2, in Ar) in order to obtain or to improve the VO_2 phase (see, for example, Refs. 12–15). Once postannealing is employed, it appears logical to make a clean separation of metal deposition and subsequent oxide-forming annealing. Some films were produced in this way, by oxidation of vanadium metal precursor films and plates in air and in oxygen-argon mixtures.[26–32] This is the method we are using in this paper. We found that this POP, upon proper optimization, produces good phase-transitioning VO_2 films.

In the past, many films prepared by POP were found to have a compositional gradient in z direction, with V_2O_5 layers at the upper surface, VO_2 in the bulk of the film, and lower oxides such as $VO_{0.5-1.0}$ near the lower interface.[31] A similar oxygen variation in z direction was found in anodic films.[24]

It should be noted that precursors other than a metallic V were occasionally used. An interesting attempt to reduce or eliminate the z gradient by annealing a more complex $V_2O_5/V/V_2O_5$ precursor sandwich structure is described in Ref. 32. In some publications the precursor is not a metal, but the highest V oxide, V_2O_5, and subsequent annealing is performed in vacuum rather than in O_2 in order to reduce it to VO_2.[33]

We felt that oxygen concentration gradient in z direction will not be present, or at least will be minimized, if the V precursor film is sufficiently thin and if oxidation proceeds slowly. The latter requires performing oxidation in reduced pressure O_2, as described below. Slow oxidation of a vanadium precursor film in reduced pressure air was described previously in Ref. 29. It appears that our films are of a somewhat higher quality, possibly due to a replacement of air with oxygen.

The drive toward thinner VO_2 films thus in part comes from the desire to minimize the compositional z gradient, but more importantly, some recently proposed applications of interest to us require VO_2 films to be in the 10 nm range.[3] Thus it is interesting to see just how thin a transitioning VO_2 film can be made. In surveying the literature we found the thinnest VO_2 films, down to 6 nm,[19] grown epitaxially on TiO_2 underlayers by metal organic chemical vapor deposition (MOCVD), exhibiting electrically measured phase transition with $RR\sim 10^2$. A recent work reports transitioning of 7–8 nm VO_2 films with $RR\sim 10^3$ grown epitaxially on TiO_2 substrates by PLD.[23] In most of the literature, however, one finds transitioning VO_2 films that are considerably thicker, from about 50 nm and up. We thus have set as one of the goals of this work to investigate how far we can push POP in producing the thinnest films still showing the phase transition.

In this paper we report on POP preparation of VO_2 films with the V precursor thickness ranging from 10 to 100 nm, which results in VO_2 thickness from about 22 to 220 nm. Below the VO_2 thickness of ~20 nm the phase transition was exceedingly weak or nonexistent, and so we do not envision pushing our POP method to even thinner films, at least not on lattice-mismatched or amorphous substrates. We note that in the future it may be of interest to test POP for ultrathin films on lattice matched substrates.

II. FILM PREPARATION: AIR AND *IN SITU* ANNEALINGS

Vanadium precursor films were deposited by rf sputtering of 6 in. diameter V metal target (99.9%) in pure argon. The chamber was pumped to about 10^{-5} Torr; after that

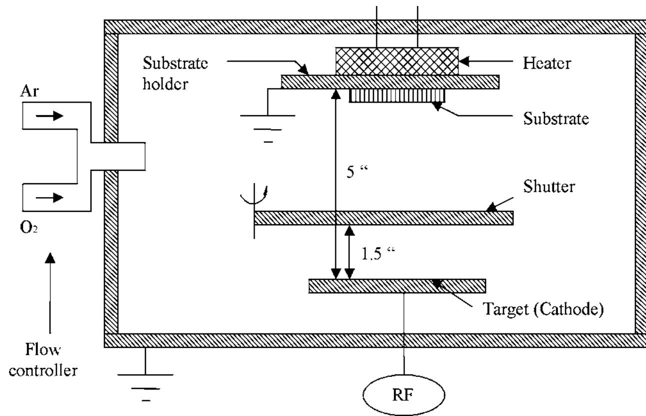

FIG. 1. Deposition chamber schematics.

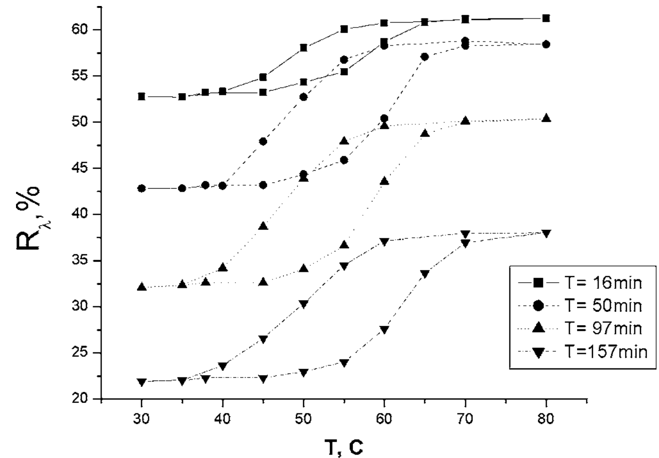

FIG. 2. Reflectivity loops $R_\lambda(T)$ measured at $\lambda=1000$ nm. The precursor V film was 80 nm thick, deposited on a Si/SiO_2 substrate. The loops were measured after the consecutive air-furnace annealings of this precursor at 350 °C, cumulative annealing times indicated in the inset.

0.75 mTorr of Ar were introduced. The rf power was in the range from 0.3 to 1.5 kW. The distance between the substrate and the target was 5 in. (sometimes, 1.5 in., when substrates were attached to a shutter, Fig. 1).

The deposition rate used for 10–30 nm precursor film depositions was ~1 nm/s, while for thicker precursor films it was ~8 nm/s. When examined after the deposition (without oxidation), V films were metallic, albeit with resistivity of $(3-5)\times10^{-6}$ Ω m, which can be compared with pure V at room temperature having resistivity of 2×10^{-7} Ω m. Apparently V, being a good getter of oxygen, absorbs it from the residual oxygen present in the chamber during the deposition; still, it is a dirty metal rather than any of the oxide phases in the VO_x series. We also checked resistivity of as-deposited Al; it turned out to be in the $(3-9)\times10^{-8}$ Ω m range, comparing with pure Al at room temperature having resistivity of 2.7×10^{-8} Ω m.

The substrates were Si wafers, Si/SiO_2 wafers, Si wafers covered with 50–100 nm of Al (Al mirror for optical interference measurements), as well as Al foil, glass, and quartz. We also successfully prepared transitioning VO_2 films on Si wafers covered with 12 μm layer of high-porosity silica *aerogel*. This work, which is relevant to the recently proposed IR imaging scheme,[4] will be reported separately.[34]

V and resultant VO_2 film thicknesses were measured by Dektak-3 ST surface profiler. The thickness uniformity of 5% was limited to about 0.5 in. diameter area on a substrate. This can be easily improved by using a substrate rotation above the cathode.

Although our best films were prepared *in situ*, it is surprisingly easy to prepare transitioning VO_2 films in air, at atmospheric pressure.[35] Here we briefly present results for air-annealed films. As a base line experiment, we verified with GIXRD (synchrotron) analysis that sufficiently hot air annealings produce the highest V oxide, V_2O_5, as expected. For example, we find pure orthorhombic V_2O_5 after only 3 min annealing at 500 °C in air. The transitioning (i.e., VO_2 containing) samples were obtained for annealing temperatures starting from 270 °C, with better quality samples annealed at 450 °C. The annealing times could be as long as several hours at the low end of annealing temperatures and as short as 1 min at 450 °C. Although we discuss optical reflectivity measurements in Sec. V below, as an example, in Fig. 2 we show a progression of hysteretic reflectivity curves $R_\lambda(T)$ measured at $\lambda=1000$ nm after a series of low-temperature (350 °C) air annealings of an 80 nm V precursor.

By virtue of exhibiting a phase transition, the data in Fig. 2 indicate that there is at least some VO_2 phase present in all of the annealed films. With subsequent annealings, the reflectivity ratio between the *M* and *S* phases increases from about 1.1 to about 1.7, presumably due to an increasing volume fraction of VO_2, while the percentage of reflected light is decreasing, presumably due to a reduction in thickness and eventual disappearance of the remaining reflecting back layer of metallic V. The loop width, if measured between the steep parts of the hysteresis loop, is about 15 °C; the full extend of the hysteresis loop, between the merging points, is about 40 °C. This is typical of thin polycrystalline VO_2 films (see below). It is also interesting that the midpoint of the hysteresis loop, which we take to be the transition temperature T_C, is approximately 55 °C here, which is considerably lower than the bulk T_C=68 °C in pure VO_2.[1] We (as well as others) often observed such T_C lowering in our films (see below). We tentatively ascribe T_C lowering to the presence of either stress, or doping (for example, by the atoms of the substrate, such as Si), or nonstoichiometry of VO_{2-x}, or all of the above. It should be noted that the annealing temperature of 350 °C is low compared to what can be found in most of the literature on VO_2 preparation.

Although it is relatively easy to prepare transitioning VO_2 films with air annealing, our best films were prepared *in situ*, in the deposition chamber, immediately following the deposition of the V precursor. The flow of ultrahigh purity oxygen was regulated with the flow controller, and the chamber was simultaneously pumped through a throttle valve to maintain a dynamic pressure of 0.200 Torr of O_2. The heater shown in Fig. 1 was used to raise the temperature of the precursor film to 370–415 °C, and the slow annealing took from 2.5 to 7 h.

- The optimum POP preparation conditions for "thick" 200-nm-range films: V precursor thickness of

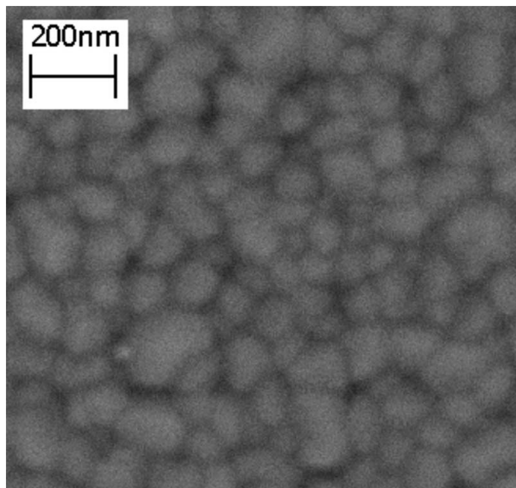

FIG. 3. VO_2 film, 220 nm thick, on a Si/SiO_2 substrate. The scale is shown on the figure. This makes the side of this photograph of ~1.4 μm length. This film had a strong SMPT with $RR=\rho_S(25\ ^\circ C)/\rho_M(90\ ^\circ C)=1920$. One can see grain structure with grains from ~50 to ~200 nm, with typical grain size of ~100 nm.

80–100 nm, annealing in dynamically maintained 0.200 Torr O_2 at 390–415 °C for 6.5 h.

- The optimum preparation conditions for "thin" 20-nm-range films: V precursor thickness of 8–10 nm, annealing in dynamically maintained 0.200 Torr O_2 at 390–415 °C for 4.0 h.

III. VO_2 FILMS MORPHOLOGY AND STRUCTURE FROM SEM, AFM, GRAZING-INCIDENCE XRD, AND RAMAN MEASUREMENTS

The theoretical ratio of the volume (i.e., thicknesses in thin films) of resulting VO_2 and precursor V is $\gamma=2.25$.[36] In Ref. 29 the films were produced by a slow annealing in reduced pressure air, similarly to our version of POP except that we anneal them in oxygen. According to Ref. 29, an experimental $\gamma=2.3\pm0.1$ was found for the 120 nm precursor V film after annealing in air at 0.08–0.25 Torr lasting for over 3 h. With our *in situ* method, we rarely measured the thickness of precursor V films. Based on V deposition rate, and confirmed by an occasional measurement, our measured γ were similar in the 2.2 ± 0.3 range.

The surface morphology of our films was studied in optical metallographic microscope, in SEM, and in AFM. In an optical microscope the films appear smooth and shiny. They have the beautiful colors for which VO_2 films are famous.

SEM provides information on the grain structure. A SEM photograph taken on one of our best films is shown in Fig. 3.

AFM measurements were performed on *Dimension 3000* with *Nanoscope IIIa Controller* (Digital Instruments, Inc.) The results are shown in Figs. 4(a)–4(c). All pictures are obtained by making the AFM microscope software present the collected surface profile data in a form of three-dimensional (3D) pictures viewed in projection. Each picture represents a $1\times1\ \mu m^2$ scan of a given surface. Note that in all the cases [(a)–(c)], the apparent z axis extend of the film does not correspond to its real thickness; all real thicknesses, which are given in the figure caption, are much greater than those apparent ones.

Figure 4(a) indicates a relatively smooth V precursor surface with rms roughness of 0.50 nm. With all 3D pictures having the same vertical scale, it can be seen that the VO_2 surfaces are getting progressively rougher with increasing film thickness, with rms roughness values increasing to 2.1 nm in a 24 nm film and to 5.2 nm in a 220 nm film. This corresponds to rms-to-thickness ratios of 2.6% in V precursor, 8.8% in a 24 nm film, and 2.4% in a 220 nm film. Further, assuming that each well-developed bump in representative line scans corresponds to a grain, we can approximately estimate average grain sizes in the three samples. We obtained grain sizes of 70 ± 20 nm in V and 100 ± 20 nm in VO_2 films. There is a satisfying agreement between this determination and the grain size visible on a SEM photograph of a 220 nm film (Fig. 3).

Grazing-Incidence XRD (GIXRD). As is well known, x-ray characterization of thin polycrystalline films is non trivial. In the GIXRD geometry, by increasing the path length of the incident x-ray beam through the film, the diffraction intensity from the film can be increased so that conventional phase identification analysis can be run. The highly collimated synchrotron beam at the National Synchrotron Light Source (NSLS) at Brookhaven National Laboratory (BNL) has been used at 2°–5° incidence angles. There is a dramatic increase in signal to the background noise ratio in such a configuration. According to these measurements, films characterized by strong phase transitions are essentially pure-phase VO_2. As an example, in Fig. 5 we show such data for a 185 nm POP VO_2 film on single-crystalline Si substrate (V precursor annealed at 370 °C for 5.5 h in 0.200 Torr of O_2).

Raman spectroscopy is recognized as a powerful tool to probe a local structural composition. We used it to evaluate our thick (220 nm) and thin (24 nm) VO_2 films on Si/SiO_2 substrates. In previous studies[37] this technique was used to successfully identify the presence of additional (non-VO_2) VO_x phases in thin films deposited on a glass substrate. At room temperature, such analysis is typically complicated by the fact that many Raman lines of vanadium dioxide are very close in their spectral position to Raman lines of V_2O_3 and V_2O_5. To avoid this confusion, a simple methodology based on measuring Raman spectrum at the temperatures below and above the temperature of the phase transition was developed.[37] This method is based on the observation that the Raman signal is heavily damped in a metallic phase, and so the Raman spectrum in VO_2 appears featureless above the phase transition temperature.[38] Thus, if non-VO_2 compounds are present in a film, their presence will be reflected in the Raman spectrum above the phase transition temperature.

We used a commercial confocal Raman microscope (Renishaw, Inc), which is spectrally and intensity calibrated. The excitation radiation at the incident wavelength of 633 nm was properly attenuated to avoid a possible local heating of a sample above the phase transition temperature. When all the incident power of the laser was used, the local temperature exceeded 100 °C, which was independently confirmed by taking the ratio of intensities of the corresponding frequency components of the Stokes and anti-Stokes Ra-

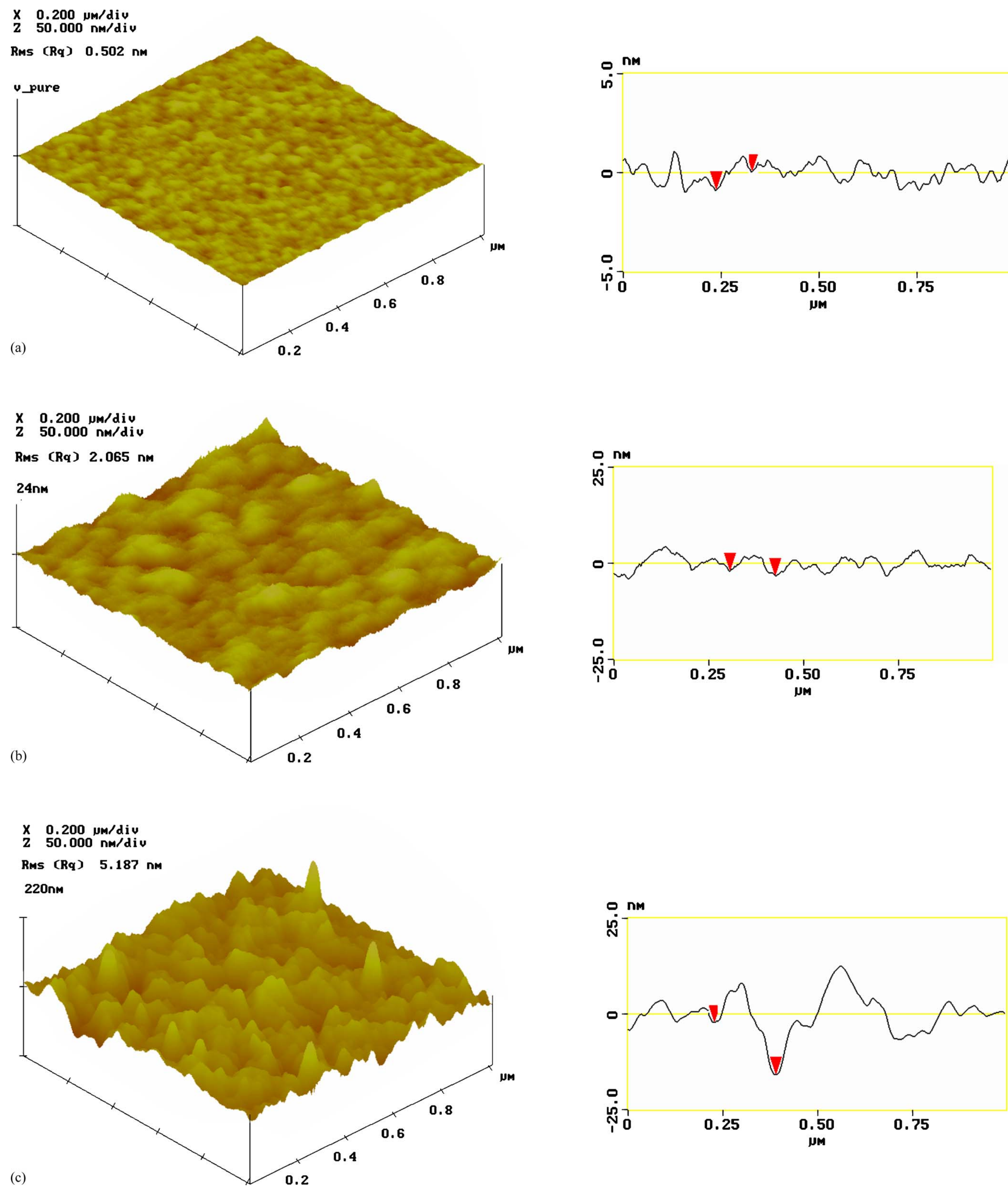

FIG. 4. (Color online) AFM 1×1 μm^2 scans in 3D representation viewed at a 45° angle, vertical scale in all 3D pictures of 50 nm/division. The average (rms) roughness figures were calculated over areas of $\sim 750\times 750$ nm^2 for each sample. Representative line scans next to 3D pictures can be used to estimate the average grain size. All films are on Si/SiO_2 substrates. (a) 80 nm V precursor film, rms roughness=0.50 nm; estimated grain size: ~70 nm; (b) 24 nm VO_2 film annealed *in situ* at 390 °C for 2.5 h, rms roughness=2.1 nm, estimated grain size: ~100 nm; (c) 220 nm VO_2 film annealed *in situ* at 415 °C for 6.25 h, rms roughness=5.2 nm, estimated grain size: ~100 nm.

man spectra.[37] Those measurements were done at several points on the surface of each sample to confirm the homogeneity of the films. Typical Raman spectra for the 220-nm-thick and 24-nm-thick films are shown in Fig. 6, where the Raman signal from the thinner sample is magnified approximately ten times to be compared with the corresponding spectrum from the thicker sample. Both spectra were recorded at the same excitation conditions at the tem-

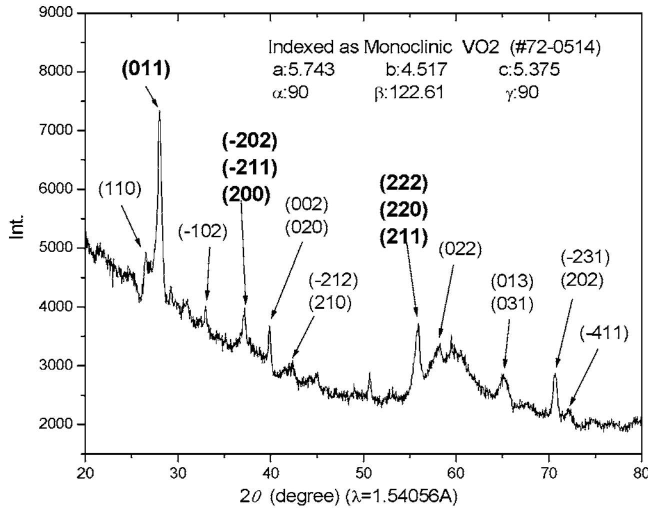

FIG. 5. Synchrotron GIXRD data, measured at an incidence angle of 5°, at 20 °C, on a 185 nm VO_x film on Si wafer substrate. Bold indices are the highest three peaks in the XRD spectrum, which are in agreement with the monoclinic VO_2 phase (JCPDS #72-0514),[55] which is the right structure for the semiconducting room-temperature phase of this material. The lattice parameters and angles are indicated on the figure. Other minor peaks indexed come from the silicon oxide, originating from the substrate.

perature at about 20 °C and showed the substantial presence of Raman lines associated with Si (300 and 520 cm^{-1}) and SiO_2 (930–1000 cm^{-1}). In the figure, Si and SiO_2 lines are labeled; all the other lines belong to VO_2 (see Ref. 37). One can also notice the dramatic difference in the position of Raman spectral lines for those two films. While, for the thicker sample, these Raman lines correspond exactly to the Raman lines of VO_2, the Raman lines recorded for the thinner sample appeared to be spectrally shifted. However, when both samples are heated above the phase transition temperature, all these lines, which are not related to the substrate, disappear signifying the association with the VO_2 phase. The absence of any significant peak at around 700 cm^{-1} also independently confirms the lack of V_2O_5 phase, which is the

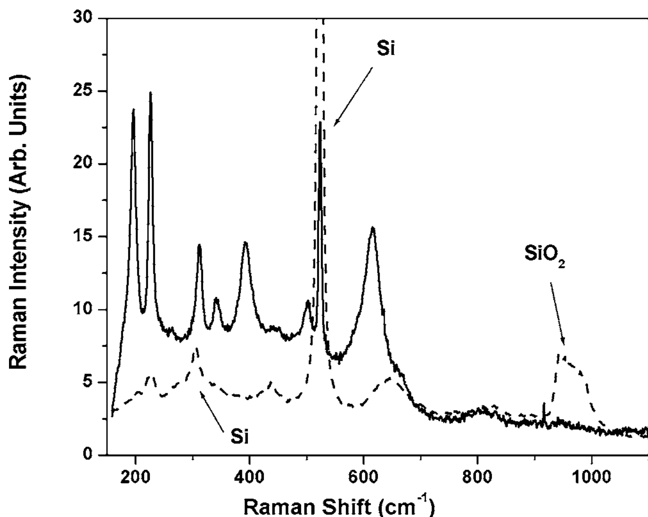

FIG. 6. Typical Raman spectra from a 220 nm VO_2 film (the solid line) and from a 24 nm VO_2 film (the dashed line), both on a Si/SiO_2 substrate. Measurements are taken at the temperature well below the phase transition temperature. All lines which are not labeled belong to VO_2.

mostly commonly occurring second phase in the VO_2 film growth. We tentatively attribute the spectral shifts of the Raman lines observed in the 24 nm film either to a greater stress or to a greater influence of surface vibrational modes.

IV. RESISTIVE TRANSITIONS, ABSOLUTE RESISTIVITIES, TCR, AND $R_\square$

The resistive phase transition, in addition to being of central interest in several applications of VO_2 films, provides a convenient test of film quality, with the transition in bulk single crystals and best epitaxial films serving as a "gold standard." In VO_2 single crystals the resistivity ratio ρ_S/ρ_M taken at the transition reaches $\sim 10^5$, and the hysteresis width ΔT_C=0.5–2 °C.[39] We note in passing that in many papers the authors seem to confuse the hysteresis width (ΔT between the heating and cooling branches) with the width of a single hysteresis branch, i.e., the width of a resistivity jump taken in a particular direction, either heating or cooling. The latter can be as sharp as 0.1 °C, while the former is significantly greater, as quoted above, even in single crystals. The best epitaxial films are quite similar to single crystals, exhibiting RR up to 10^5 and ΔT_C of 1–2 °C.[16,20–23] Nonepitaxial polycrystalline films typically have broadened hysteresis width $\Delta T_C \sim 10$ °C, where ΔT_C is defined as an interval between the points of the steepest slope in the hysteresis loop. In polycrystalline films ΔT_C should be distinguished from a greater full width of the loop $\Delta T_L \sim 40$ °C, defined as an interval between the merging points. While the RR in bulk single crystals and in the best epitaxially grown single-crystalline films can be defined right at the transition, in polycrystalline films, large ΔT_L does not allow for a convenient measurement at or around the T_C. In this paper we define RR as calculated between ρ_S (25 °C) and ρ_M (90 °C), which seems to be the prevailing, if unspoken, definition in the literature on VO_2 polycrystalline films. This is a convenient temperature interval to compare films with hysteresis loops of various widths, as most of them do not have hysteresis extending beyond 25 and 90 °C. However, we note that because of the semiconducting nature of $\rho_S(T)$, this definition overestimates the actual jump of resistivity in the vicinity of the phase transition. For example, if single crystals were characterized by the so-defined RR, it would reach over 10^6.[39]

In order to measure film resistivity, we used the four-probe geometry defined with the use of a shadow mask during V precursor deposition. The mask defined a film strip of 1 mm wide, with the distance between voltage leads of 2 mm. By virtue of our *in situ* method, the mask remained in place also during the precursor oxidation stage. We made sure that the use of this mask did not significantly change film properties by comparing these films with others deposited without a mask.

We checked current-voltage proportionality in our four-probe measurements, to make sure that our measurements are meaningful, reflecting intrinsic properties of VO_2 rather than current-induced heating effects and resulting interplay of the S and M phases. As other authors before us,[2,40] we found that in film VO_2 samples, in a high-resistivity S phase,

it is easy to exceed currents exhibiting linear *I-V* (Ohmic) behavior. In our 200 nm films, we found noticeable deviations from linearity already at currents above 0.05 μA, which in our geometry corresponds to longitudinal fields between voltage probes $\geqslant$300 V/m. At currents over 1.5 μA, we observed S-shaped *I-V* characteristics at room temperature, which are typical of heating effects. At still larger currents we observed switching between *S* and *M* phases. The appearance of *I-V* nonlinearity indicates formation of nonuniform metallic regions in nominally semiconducting VO_2 films; of course, proper resistivity measurements should be done in the Ohmic *I-V* range.

In some resistivity measurements we mounted our samples on a flat heater and used needle probes placed on a film surface; in other measurement we used commercial Janis cryostat (model VPF-475). In the cryostat, samples were mounted on a copper block which could be heated by a heater. In all such measurements the rate of temperature change was established using a thermocouple with the temperature controller. As the film facing room temperature environment was heated through the substrate, from the back, we had to minimize lagging between the actual film temperature and the temperature measured by the thermocouple. In order to avoid this problem, we placed thermocouple on the film surface and conducted temperature sweeps at a rate of 0.5 K/min or less. We found that at faster sweeping rates the curves shifted, indicating said lagging. In the most precise measurements, we found very slow resistivity drifts (see below in Sec. VI) which may be interpreted as thermocouple-sample temperature equalization on a scale of ~0.1 °C over time periods of approximately hours.

We measured $\rho(T)$ in our typical 200-nm-range and 20-nm-range films. Not surprisingly, the former shows a much stronger (higher RR) phase transition, as can be seen in Figs. 7 and 8.

A. Absolute resistivities

It is always very useful to know absolute values of resistivity rather than just resistance and RR. Unfortunately, in the literature on VO_2, when absolute resistivity is reported at all, one finds a wide range of values differing (in different papers) by more than two orders of magnitude (!) in a given phase, making it difficult to zero in on the true intrinsic resistivity, and making a detailed review of the published data somewhat impractical. There is no doubt that part of this diversity is the result of the notorious difficulty in reproducing stoichiometric and well-ordered VO_2. For example, oxygen defects can produce different resistivities in nominally similar samples. In bulk crystals there is additionally a problem of hard-to-detect microscopic cracks, which can lead to a false determination of high apparent resistivity. In films, properties depend on a number of factors, which, in turn, depend on the thickness. Despite all these difficulties, we want to compare data on absolute resistivities in our POP films with the literature, as best we can. Therefore, below we provide resistivity ranges we found in the literature for bulk crystals, epitaxial films, and polycrystalline films. In view of what is said above, these numbers should be treated with caution, and our references, while representative, are incomplete. We also note that the ranges given below, wide as they are for a given material in a given phase, still exclude some maverick values which seem too low or too high.

The literature on bulk single crystals of VO_2 is rather limited. In it we found (in some cases reading the values from a published figure of conductivity versus $1/T$) values of

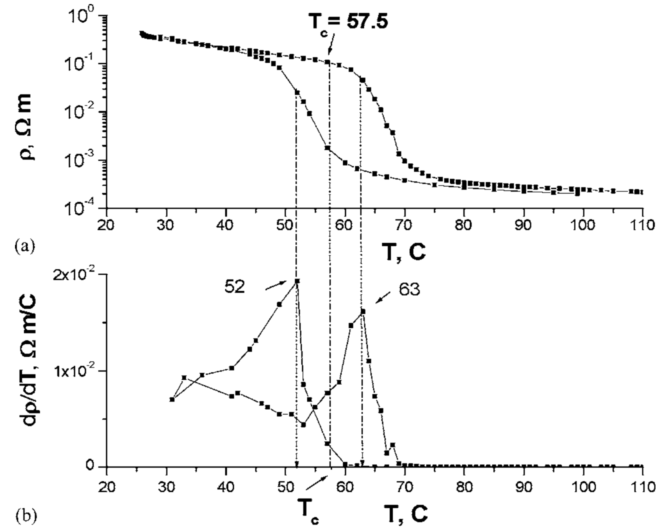

FIG. 7. (a) log ρ vs T in a 220 nm POP film on a Si/SiO_2 substrate; the V precursor was annealed *in situ* for 6.5 h at 415 °C. RR $=\rho(25\ °C)/\rho(90\ °C)=1920$; TCR can be found by taking the slope of log $\rho(T)$ and multiplying it by 2.3. (b) $d\rho/dT$ exhibits two peaks; the distance between them is taken as the width of the hysteresis loop $\Delta T_C=11\pm1$ °C; the midpoint between the peaks is $T_C=57.5\pm1$ °C (lower than the bulk value of 68 °C). Note that because of the log scale, the peaks in $d\rho/dT$ do not correspond to the max slopes of log $\rho(T)$.

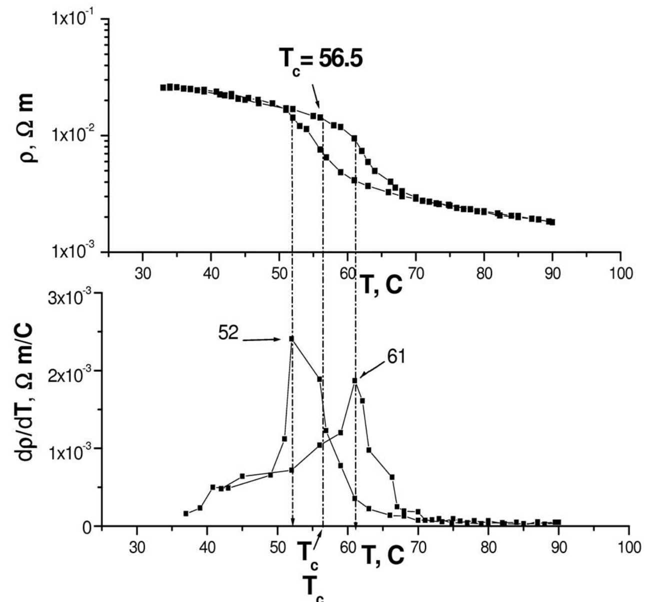

FIG. 8. (a) log ρ vs T for a 24 nm POP film on a Si/SiO_2 substrate; the film was annealed *in situ* for 2.5 h at 390 °C; RR$=\rho(25\ °C)/\rho(90\ °C)=14.5$. TCR can be found by taking the slope of log $\rho(T)$ and multiplying it by 2.3. (b) $d\rho/dT$ exhibiting two peaks; the distance between them is taken as the width of the hysteresis loop $\Delta T_C=9\pm1$ °C; the midpoint between the peaks is $T_C=56.5\pm1$ °C (lower than the bulk value). Note that because of the log scale, the peaks of $d\rho/dT$ do not correspond to the max slopes of log $\rho(T)$.

resistivity in a semiconducting phase $\rho_S(25\ °C)$ ranging from $\sim$0.2 to $\sim$12 Ω m, with "typical" values reported to be $\sim$1 Ω m.[39] In the metallic phase, $\rho_M(90\ °C)$ in bulk single crystals range from 1.8×10^{-6} to 6.3×10^{-6} Ω m.[39,41,42] The literature on epitaxial films is more extensive than that on bulk crystals; however, as mentioned above, absolute resistivity is not always reported. Except for a recent publication,[22] the values of $\rho_S(25\ °C)$ in epitaxial films that we found are significantly lower than in bulk crystals, being typically in the 1.5×10^{-3}–7×10^{-2} Ω m range. In Ref. 22, however, $\rho_S(25°\ C)\approx0.8$ Ω m, as high as in typical bulk single crystals. Values of $\rho_M(90°\ C)$ in epitaxial films are in the range of 2×10^{-7}–1×10^{-5} Ω m.[22,42–44]

In the extensive literature on polycrystalline films, when absolute resistivites were reported, we found most values of $\rho_S(25\ °C)$ between 6×10^{-3} and 7×10^{-2} Ω m and most values of $\rho_M(90\ °C)$ between 1×10^{-5} and 1×10^{-4} Ω m.[10,48]

In our optimized POP 200-nm-range films, we found $\rho_S(25\ °C)$ from 0.1 to 0.85 Ω m, with typical values of 0.4 ± 0.2 Ω m (see Figs. 7 and 14). We find this result to be quite remarkable, as these values are considerably higher than in all publications on polycrystalline films and in most publications on epitaxial films (the only exception being Ref. 22 which gives values very similar to our best values) while being very close to the typical bulk single-crystalline values.[39] We take this as an additional impressive confirmation of the quality of our films, which can be attributed to the gentle, slow oxidation process we are using in POP. In the metallic phase, we are measuring values of $\rho_M(90\ °C)$ from 2×10^{-4} to 8×10^{-4} Ω m, corresponding to RR in the interval from 500 to 2000, with prevailing numbers in the vicinity of RR=1500. Our $\rho_M(90\ °C)$ are therefore somewhat higher than the typical metallic phase values in most of the literature on polycrystalline VO_2 films.

As was said above, a similar slow oxidation, but in air, was performed in Ref. 29. From the conductivity plots in that publication, we inferred maximum $\rho(25\ °C)\approx0.07$ Ω m, with the best $RR=\rho(25\ °C)/\rho(90\ °C)\approx550$.

B. Temperature coefficient of resistance (TCR) and $R_\square$

We also measured $TCR=1/\rho(d\rho/dT)$ and resistance per square $R_\square$ $(25\ °C)=\rho/d$, where d is film thickness. These are parameters of interest in the significant military and commercial application of VO_x $(x\approx2)$ in uncooled (ambient temperature) IR imaging systems. This application does not utilize the phase transition at all.[45,46] Instead, it requires a combination of sufficiently high TCR and sufficiently low pixel (square) resistance at or near room temperature. Room temperature values of TCR from about −0.015 to −0.06 (or from −1.5% to −6%) were reported.[12–14,32,47–49] The sufficiently low resistance appears to indicate $R_\square$ in the range of 20–100 kΩ (depending on the paper); however, the authors actually involved in full IR imager development and manufacturing require $R_\square\approx20$–25 kΩ.[46,47] When quantitative data on ρ and $R_\square$ are available alongside TCR (which is not always the case in the literature), this restriction on $R_\square$ seems to limit the practically useful films to those with TCR of $\sim$2%.

As explained above, our films were optimized to have high RR (strong SMPT) and a correspondingly high $\rho_S(25\ °C)$, which implies high $R_\square=\rho_S(25\ °C)/d$. Indeed, the values of $R_\square$ in our optimized films are in the megaohm range, varying from 0.5 to 4.2 M$\Omega/\square$. The TCR in these films was from −3% to −5%. However, the high $R_\square$ values probably make them unusable for the resistive-readout IR imaging application.

V. REFLECTIVITY

In reflected white light, there is a strong color change as a VO_2 film goes through the transition (thermochromism), especially when the film is placed onto a well-reflecting surface, such as Al or V. This optical transition can be monitored and quantified with reflectance spectrometer, and the parameters of the optical hysteresis loop can be used for film quality characterization. This change in reflectance is of interest in some applications of VO_2, for example, in the proposed IR detection scheme[4] and in the proposed VO_2-based display.[50]

The thin-film interference arrangement comprising VO_2 film and a metal (typically Al) mirror underneath was used in numerous studies and optical applications of VO_2,[2] starting probably with the work of Duchene,[51] who described what he called "a dichromic display" based on this structure. The underlying physics is based on destructive interference of light reflected from the two film surfaces. With the index of refraction of Al mirror underneath VO_2 being higher than that in VO_2, both interfaces produce a π shift which can be thus neglected. In each phase with its respective index of refraction n (n_S in a semiconducting phase, n_M in a metallic phase), reflectivity exhibits a deep minimum as a function of wavelength λ_0 when $N+1/2$ wavelengths $\lambda=\lambda_0/n$ are fitting into an optical path inside the material, where $N=0,1,2,\ldots$. At normal incidence, the condition becomes $2d=(N+1/2)\lambda_0/n$, or, for the wavelength corresponding to a minimum in reflectivity $\lambda_{0\ \min}=2nd/(N+1/2)$. In Fig. 9(a) we show reflectivity versus wavelength for an 80 nm VO_2 film deposited by POP on an Al mirror (on Si wafer substrate). These data were measured with Perkin-Elmer's UV/vis spectrometer "Lambda 20." We can see the principal features of $R_T(\lambda_0)$ as described above, including the two minima. By independently measuring the film thickness d and determining from these data the wavelengths of the two minima $\lambda_M=714$ nm and $\lambda_S=829$ nm, we can calculate the refractive index n in the two phases. Solving for n, we obtain

$$n=(N+1/2)\lambda_{0\min}/(2d). \qquad (1)$$

Taking $N=0$ (half-wave fitting into $2d$) we obtain $n_S=2.59$ and $n_M=2.23$. These numbers are in good agreement with the published measured values of n in the two phases of VO_2 films (see Ref. 52 and further references given there). The dips in the curves are wide due to significant absorption (losses) in VO_2.[2] Reflectivity is smaller than 100% for the same reason, and, in general, the curves do not come all the

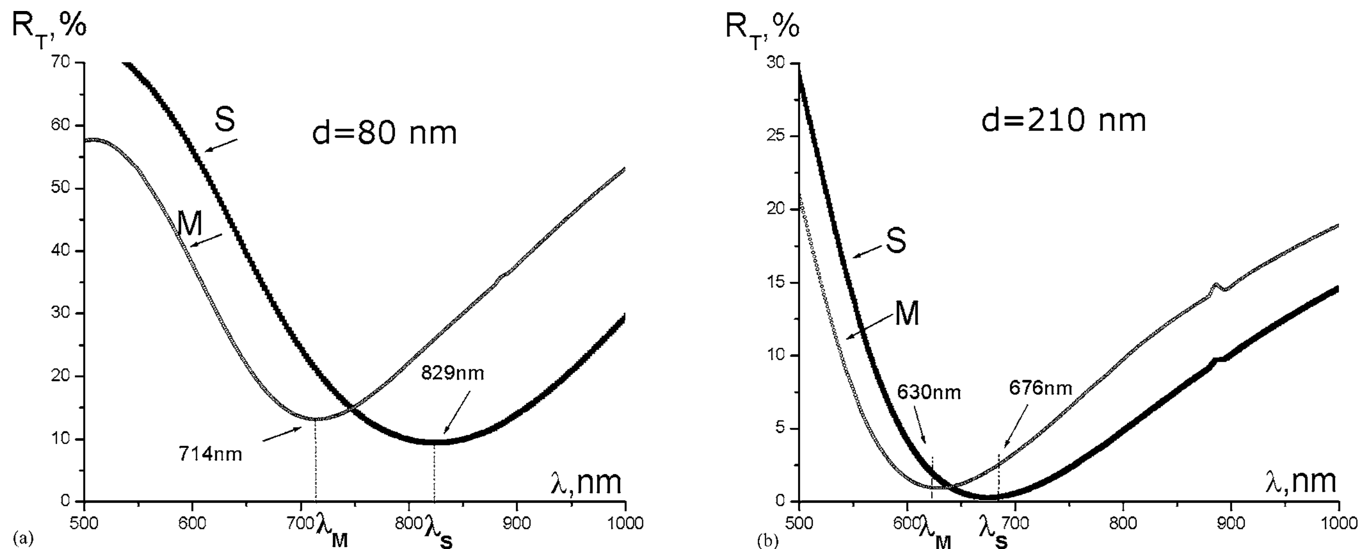

FIG. 9. R_T vs λ in the two phases, *S* and *M*, for the (a) 80 nm VO_2 and (b) 210 nm VO_2 films. Both films were deposited onto a 120-nm-thick Al mirror on a Si substrate. The wavelengths at which R_T has minimum values are indicated on the figures.

way down to $R=0$ at the minima since, with considerable absorption of the refracted beam inside the film, reflected intensities from the two surfaces are not necessarily equal.

In Fig. 9(b) we show similar $R_T(\lambda)$ data for a thicker $d=210$ nm film. In this case, while the reflectance is generally smaller (more light absorbed in the film), the minima are deeper, with minimum R_T values closer to zero, indicating a case of a more precise intensity cancelation between the two reflected beams, i.e., a more complete case of destructive interference. In this case we cannot take $N=0$ (half-wave fitting into the optical path) in formula (1), as it would produce unphysical $n<1$ values. Taking $N=1$ (which corresponds to one and a half wave fitting into $2d$) and substituting values $\lambda_M=630$ nm, $\lambda_S=676$ nm, and $d=210$ nm into Eq. (1), we obtain $n_S=2.41$ and $n_M=2.25$, also in fair agreement with the 80 nm film result and with the literature.[2,52] Note that in a 210 nm film, the wavelength shift Δλ between the reflectivity minima is smaller than in an 80 nm one, as expected.

An alternative measurement is that of $R_\lambda(T)$ at fixed λ. The hysteresis loop orientation depends on the choice of a fixed wavelength: as can be seen in Fig. 10 (and as could be deduced from examining Fig. 9), the loop will invert for the two wavelengths corresponding to the two minima. One can get more exotic loop shapes by choosing intermediate $\lambda_M<\lambda<\lambda_S$.[2]

Our measurements illustrating these two types of hysteresis loops are shown in Figs. 10 and 11 for films 185 and 24 nm thick.

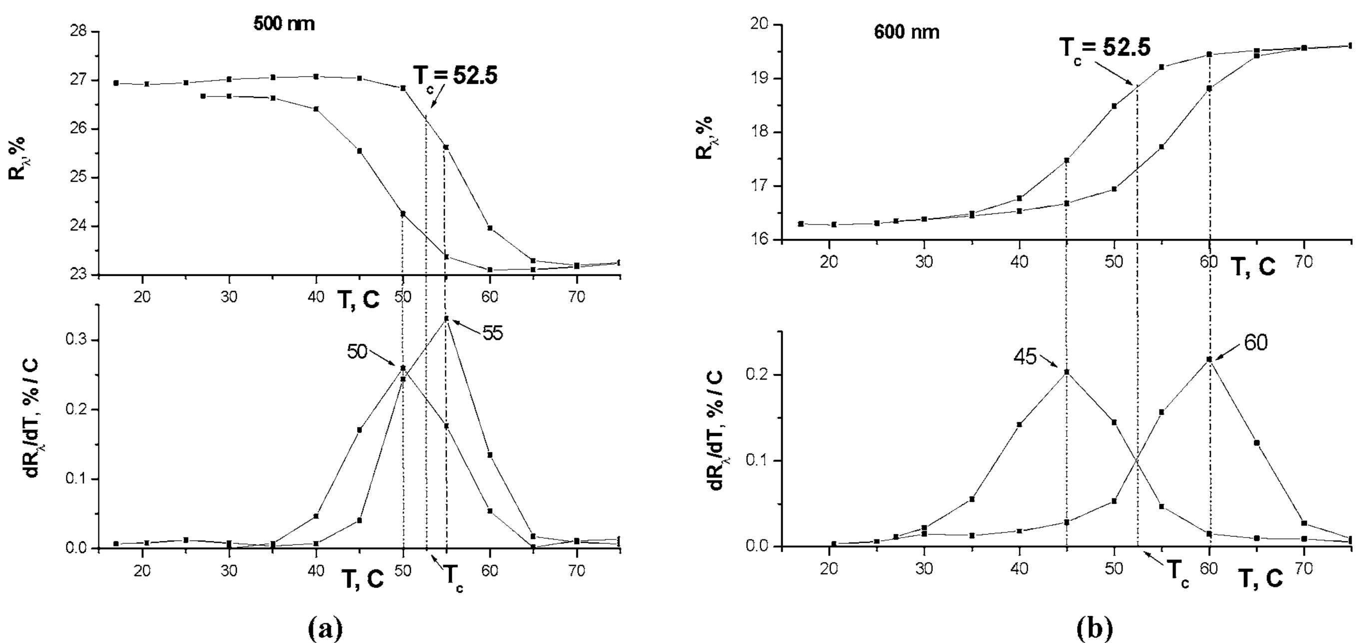

FIG. 10. (a) $R_\lambda(T)$ at fixed $\lambda=500$ nm and (b) $R_\lambda(T)$ at fixed $\lambda=600$ nm. An 80 nm V precursor annealed in 0.2 Torr O_2 for 5.5 h at 370 °C; resultant VO_2 thickness of 185 nm.

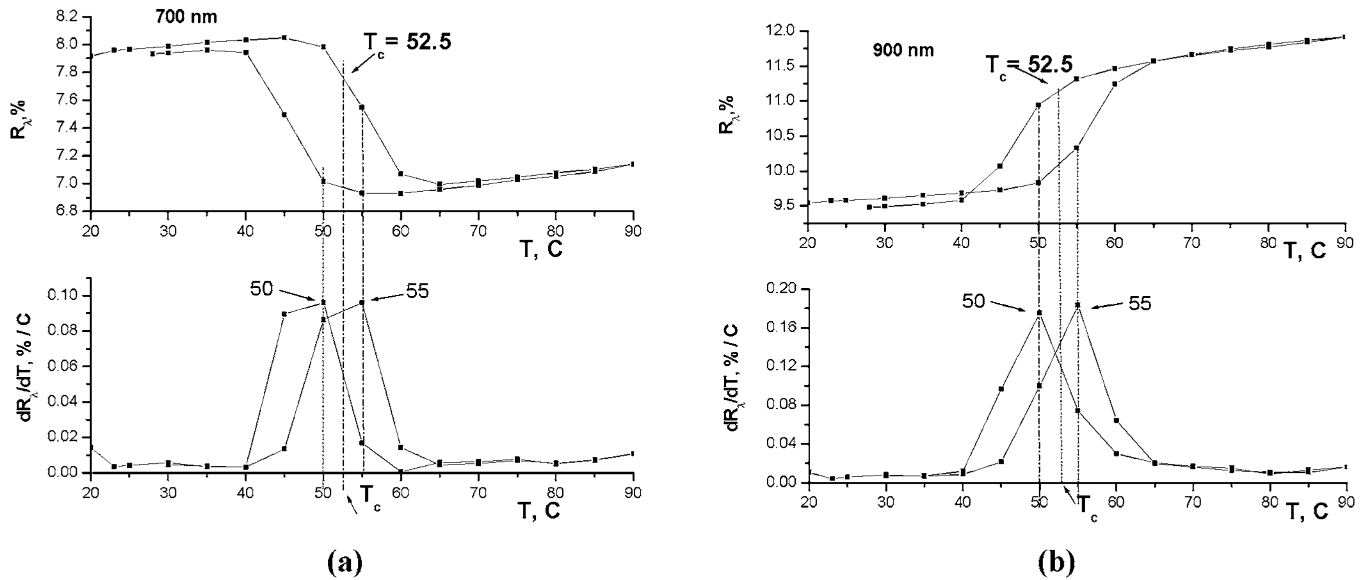

FIG. 11. Reflectivity R_λ vs T at (a) fixed $\lambda = 700$ nm and (b) at $\lambda = 900$ nm. A 16 nm V precursor annealed in 0.2 Torr O_2 for 2.5 h at 390 °C; resultant VO_2 thickness of 24 nm.

VI. REPRODUCIBILITY, TEMPERATURE CYCLING, AGING, LITHOGRAPHIC PROCESSING, AND STABILITY OF MEASURED CHARACTERISTICS IN THE HYSTERESIS LOOP

Here we report on our limited studies of POP VO_2 film characteristics in terms of the issues listed in the section title. The characteristics described in this section are mostly of interest in applications. Together with the quality of the resultant product (which was described in other sections of this paper), they are essential in determining whether a given method of film preparation will be viewed as valuable or will be abandoned.

First, a method of film preparation is required to give reproducible results, meaning that nominally identical preparation conditions lead to similar product characteristics. The degree to which this requirement, as well as a closely linked requirement of uniformity, has to be fulfilled depends on the material in question and on the intended application. As is well known, VO_2 is not the easiest material in the world to work with: it exists in a narrow range of oxygen stoichiometry, and, even at room temperature, it is not very stable with respect to oxygen composition and oxygen defects (vacancies). At the same time, SMPT is extremely sensitive to composition and structure, making it particularly hard to keep transition characteristics stable. However, insofar as this can be done with VO_2 at all, our experience with POP gives us confidence that it is a fundamentally reproducible method. Indeed, its simplicity by itself suggests that it can be done reproducibly. Keeping nominally identical preparation conditions, such as chamber vacuum, precursor magnetron deposition settings (precursor deposition rate, deposition time), backfilled oxygen flow rate and throttle-valve setting, annealing heater temperature, and annealing time, we made a number of optimized 200-nm-range films with $500 < \mathrm{RR} < 2000$, $\rho_S(25\ °\mathrm{C}) = 0.4 \pm 0.2\ \Omega$ m, reproducible reflectivity characteristics. Of the deposition parameters listed above, the essential ones are only four: precursor thickness, oxygen pressure during annealing, annealing temperature, and annealing time. All the other conditions are less important. It is not difficult to maintain good control of these four essential parameters. Looking forward, clearly the POP can be further improved in both reproducibility and uniformity; we see no principle obstacles in this direction. This can be compared with more sophisticated, multiparameter preparation methods such as reactive magnetron sputtering, reactive ion-beam sputtering, PLD, and MOCVD, where—we suspect—achieving these goals may be more difficult.

Second requirement for a practical method of film preparation is that resultant films are sufficiently stable, can be stored and processed without significant degradation. Again, the material in question will have its own limitations in this regard, but a preparation method plays a role too, especially in oxide films. For example, one preparation technique may leave more unstable oxygen vacancies in the resultant film than the other. We therefore also studied stability of our films with respect to aging, repeated temperature cycling, and standard lithographic photoresist and wet-etch processing. All these treatments were followed by measurements of resistive and optical reflectivity characteristics between 25 and 90 °C. We also studied stability of film characteristics at a fixed temperature inside the hysteresis loop.

Instrumental uncertainty in resistive and reflectivity measurements. Before we can discuss various stability measurements in VO_2, it is necessary to establish the instrumental uncertainty and temperature stability of our measurements, in general. To do so we measured aluminum and silicon "standards" which are not expected to show any instability of their own.

Instrumental limits on resistivity. We measured a 300 nm Al film at room temperature (four-probe measurement with $I = 1.0$ mA) and found over a period of 5 h resistance variations of about 0.05% or five parts in 10 000.

Instrumental limits on reflectivity. We monitored optical reflectivity of an aluminum film at 650 nm, which was kept

in the Lambda 20 spectrometer at 76±0.05 °C for 5 h. During the first 2 h we observed a continuous decrease in R_λ from 99.8% to 99.6%, i.e., a change of 20 parts in 10 000. In the last 3 h the slow drift has ceased. On top of this slow drift and, generally, all through this measurement, we recorded fluctuations (noise) on the level of about 0.03%–0.05% or three to five parts in 10 000. We found a similar slow steady decrease in reflectivity of Si/SiO_2 wafer over a period of 3 h amounting to 46 parts in 10 000, with similar noise level. Such were the instrumental stability and noise levels of reflectivity measurements in our spectrometer.

Stability of film characteristics inside the hysteresis loop. Much of our data and our general interest in VO_2 (Refs. 3 and 4) have to do with the SMPT and with the measurements inside the hysteresis loop, where the two phases, S and M, coexist in small, nanometer-scale domains, or grains.[2,53,54] As the temperature changes, the fraction of grains in one phase grow at the expense of the other. It has been incurred that domain or grain boundaries are themselves mobile during the phase transition. This suggests that even at a fixed temperature, there may be some grain-related dynamics at work which can manifest itself as instability of a given physical characteristic inside the hysteresis loop. One can, in principle, observe time drift and/or fluctuations (noise) in a measured physical quantity such as resistivity or reflectivity even at a fixed temperature. While a serious study of this issue requires noise power spectrum measurements as a function of frequency, which we have not performed, as a base line experiment, we did attempt to get some information by measuring resistivity and reflectivity at a fixed temperature as a function of time.

We monitored resistivity in the hysteresis loop of 300 nm VO_2 film at $T=60\pm0.05$ °C; this temperature was fixed on the cooling branch. The nominally constant temperature was maintained with the use of a temperature controller connected to a thermocouple. The overall data were similar to Fig. 7, although the hysteresis loop in that sample was shifted to higher temperatures by a few degrees. At this fixed temperature, the four-probe measurement of film resistivity, using measuring current $I=0.500$ μm, exhibited resistance drift of 2.5% or 250 parts in 10 000, in 7.5 h. According to the temperature controller specs, it can maintain sample temperature within an interval of ~0.1 °C, and this is what we indeed observed, with temperature readings changing by not more than 0.1 °C once a constant temperature was established. Looking at our $\rho(T)$ data, we saw that at 60 °C we should expect ~40% change in resistivity per degree or about 4% per $\Delta T=0.1$ °C. Therefore the observed considerable resistivity variation could come entirely from small temperature variations at a nominally constant temperature. The fact that resistivity tended to drift in one direction (increasing with time) may be viewed as suspicious in a sense of a sample actually changing its properties at a given T, or it can be explained by assuming that the sample temperature was slowly lowering by about 0.1 °C during this prolonged measurement. While this requires further investigation, we tentatively conclude that within the precision of our measurements, at a nominally constant temperature within the hysteresis loop, resistivity of our VO_2 film does not provide strong evidence for additional time-dependent phase dynamics or domain switching.

When we continually measured reflectivity at a fixed wavelength $\lambda=828$ nm in a VO_2 film on silicon at 76±0.05 °C (inside the hysteresis loop), we found that over a period of over 4 h reflectivity in the hysteresis loop was slowly (hours) oscillating between 21.1% and 21.14%, i.e., the relative change in absolute reflectivity was about 20 parts in 10 000, while noise fluctuations in reflectivity were limited to about 0.01%, i.e., to about five parts in 10 000. We also monitored reflectivity of a VO_2/Al sample (VO_2 on aluminum mirror), which has higher reflectivity than VO_2 on silicon. The VO_2/Al sample was measured at 650 nm while maintained inside the reflectometer at $T=76\pm0.05$ °C for a period of 4.5 h. This time we observed a steady gradual decrease in reflectivity from 47.6% to 47.35%, i.e., by about 50 parts in 10 000 in terms of absolute reflectivity, and noise fluctuations on the level of 0.02% or about four parts in 10 000. Comparing these numbers with the aluminum standard measurement described above, we conclude that these changes are consistent with our instrumental resolution and therefore are unlikely to result from the domain dynamics in VO_2.

Thus, to the limits of our temperature control and our instrumental resolution, and taking into account steep $\rho(T)$ dependence in VO_2, the long-term (hours) constant-temperature measurements of VO_2 inside the hysteresis loop both in resistivity and in reflectivity do not bear evidence of $S \leftrightarrow M$ phase dynamics.

In repeated temperature cycling, we observed resistivity returning to its initial value at room temperature to within 1%–2%. However, at 90 °C, in the metallic phase, resistivity tended to fluctuate from run to run by as much as 12%.

Aging: We measured reflectivity $R_\lambda(T)$ and then remeasured it in a film which was kept in ambient room atmosphere without any special precautions for a period of 11.5 months. We observed a consistent ~4% increase in reflectivity after this time. Simple remeasuring of reflectivity without aging produces a significantly smaller ~1% scatter. The results are superimposed in Fig. 12, with the ~4% shift eliminated in order to show the reasonably close matching of reflectivity curves (it can be seen that the aged curve is also shifted to higher temperatures by about 2 °C). With reflectivity being sensitive to the film's surface, it is possible that the observed change had to do with real surface changes due to additional oxidation and/or other surface modification. It is, however, surprising that reflectivity have increased rather than decreased after the storage. It is more likely that the observed shift arose due to recalibration of the reflectivity measuring system, which was done in the meantime, with the standard Al mirror reflection taken as 100%. These recalibrations, in fact, tend to readjust absolute reflectivity by about the same amount of 4%–5%.

Lithographic processing: We also defined some simple patterns on our films using standard lithographic processing involving spinning of the resist, baking of the resist at 90 °C for 1 h, lift-off in acetone, and wet etching in diluted acids. We adopted known etching recipes[35] and further developed

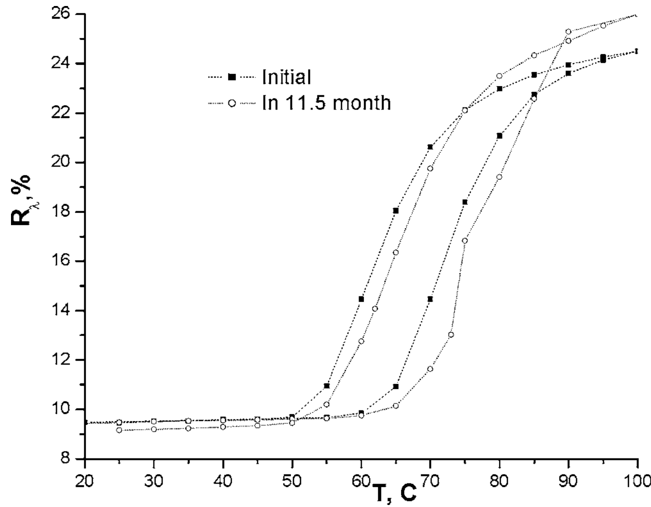

FIG. 12. Aging effect on reflectivity of an 80 nm VO_2 film on a 120 nm Al mirror: reflectivity remeasured after 11.5 month (open circles) superimposed on the initial reflectivity curve (solid squares). The initial reflectivity was shifted up by 3.5%. The film was stored in normal room ambient.

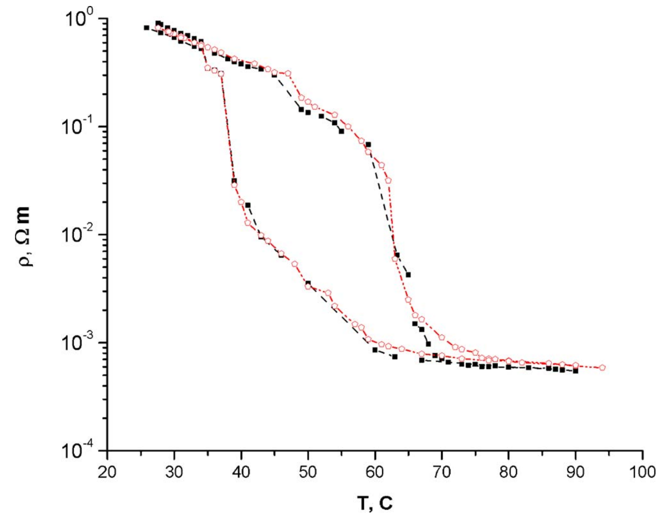

FIG. 14. (Color online) Resistivities of a 270 nm film before (solid squares) and after (open squares) photoresist processing which involves covering it with resist, backing resist for 1 h at 90 °C, and resist stripping in acetone.

recipes for selective wet etching of VO_2 and wet etching of VO_2/Al bilayer films. If we wanted to etch only VO_2, we used diluted nitric acid etch, which etches VO_2 but does not etch Al. If we wanted to etch both VO_2 and Al, we used the mixture of phosphoric, nitric, and acetic acids in water, in the ratio of 16:1:1:2. In Fig. 13 we show an optical photograph of a VO_2 line on a Si substrate defined in this way. As can be seen, the line is smooth and well formed.

Resistivities in a 270 nm film before and after photoresist processing are shown in Fig. 14. As can be seen, the curves are very similar when plotted together on a log $\rho(T)$ vs T plot. On the linear scale, the largest deviation, an increase of about 36% after processing as compared to resistivity before processing, occurred in the metallic phase at about 70 °C; at 90 °C it is about 10%. Note the high RR $\sim$1500 and the high resistivity of 0.85 Ω m at 25 °C. The bumpy hysteresis loop seen in Fig. 14 is observed in some samples; it can be attributed to sample nonuniformities between the measuring voltage probes (distance of about 1 mm here).

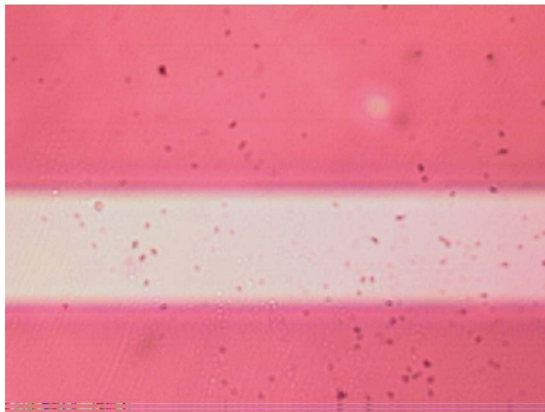

FIG. 13. (Color online) Optical photograph of a 20 μm line defined in POP VO_2 film with standard photolithography and wet etching.

VII. SUMMARY

We described a rather straightforward two-stage method for the preparation of good quality VO_2 films, the precursor oxidation process (POP). This method is not new (see, for example, Ref. 29), but we optimized it to produce good quality films. In the first stage, metallic vanadium precursor is deposited onto a substrate, and in the second stage a slow (4–6.5 h) *in situ* annealing of that precursor is performed in 0.2 Torr of O_2 at the annealing temperature from 390 to 415 °C. The thickness of the resulting VO_2 film is approximately twice greater than the V precursor thickness. We studied VO_2 films with thickness from 24 to 220 nm. All POP films are optically smooth, with SEM and AFM measurements revealing grainy structure with rms surface roughness incurred from AFM of 2 nm in the 20-nm-range films and 5 nm in 200-nm-range films. The average grain size in 220 nm films is about 100 nm, from both SEM and AFM. Judging by the x-ray diffraction and Raman spectroscopy, our films are essentially a pure-phase VO_2. The Raman lines in the 200-nm-range films are exactly as expected for VO_2, while the positions of Raman peaks in a 24 nm film were shifted, which is tentatively ascribed to stress or to the influence of surface vibrational modes in a thinner film. In the 200 nm range, POP reliably and reproducibly produces films undergoing a strong SMPT with resistance ratio RR $\approx$500–2000 (prevailing RR$\sim$1500), $\Delta T_C \approx 11$ °C, and absolute values of resistivity in the semiconducting phase which are almost as high as in the best bulk single crystals, typically $\rho_S(25\ °C)=0.4\pm0.2\ \Omega$ m (Fig. 7; we measured 0.85 Ω m in one sample, Fig. 14). These resistivity values in S phase are higher than in any other VO_2 thin film reported in the literature, including epitaxially grown oriented films [with one exception of $\rho_S(25\ °C)=0.8\ \Omega$ m in Ref. 22]. Thinner films in the 24 nm range exhibit weaker transitions with RR$\approx$15. Phase transitions are also observed in optical reflectivity in films with thickness from 80 to 220 nm. Interference measurements on our films allowed us to determine indices of refraction in the two phases, and the results agree

well with the literature. Both resistive and optical transitions serve as ultimate quality test of VO_2 films, and both transitions may find valuable applications. POP results are reproducible, and films are sufficiently stable against ambient storage, thermal cycling, and standard lithographic resist processing. Resistivity and reflectivity at constant temperature inside the hysteresis loop are stable within the instrumental resolution of our measurements, suggesting that the balance of the mixed *S* and *M* phases in the hysteresis region is not spontaneously shifting at a fixed temperature. We ascribe good film qualities to the benefit of slow oxidation employed in our version of POP.

ACKNOWLEDGMENTS

This work was partially supported by the New York Center for Advanced Sensor Technology (Sensor CAT) and partially with the Stony Brook-BNL joint research seed grant. We are greatly indebted to Professor Felix Chudnovskyi for inducing our interest in the VO_2 phase transition and its applications, and for his contributions to this work, including teaching us how to make VO_2 films by postannealing in air and advice on etching solutions. We thank Yulei Weng for her work on developing selective etching solutions and for photolithographic processing of our films. We thank Dr. M. Gouzman for his continuous assistance with instrumentation and measurements. We thank Professor G. Belenky for his interest in this work and for the use of his e-beam deposition system and Professor M. Rafailovich for her support and the use of her AFM facility. We are also grateful to Dr. Peter Shkolnikov, Deputy Director of Sensor CAT, for his continuing support and interest in this work.

[1]F. J. Morin, Phys. Rev. Lett. **3**, 34 (1959); N. Mott, *Metal-Insulator Transitions* (Taylor & Francis, London, 1997).
[2]A. A. Bugaev, B. P. Zaharchenia, and F. A. Chudnovskyi, *Metal-Semiconductor Phase Transition and its Applications* (in Russian, Nauka, Leningrad, 1979) [*Semiconductor Physics* (Consultants Bureau, New York, 1986)].
[3]F. Chudnovskyi, S. Luryi, and B. Spivak, in *Future Trends in Microelectronics: The New Millennium*, edited by S. Luryi, J. M. Xu, and A. Zaslavsky, (Wiley Interscience, New York, 2002), pp. 148–155.
[4]F. Chudnovskyi, M. Gurvitch, and S. Luryi, WIPO Publication No. WO/2002/099896 (available online from World Intellectual Property Organization at http://www.wipo.int/pctdb/en/).
[5]E. N. Fuls, D. H. Hensler, and A. R. Ross, Appl. Phys. Lett. **10**, 199 (1967).
[6]G. A. Rozgonyi and D. H. Hensler, J. Vac. Sci. Technol. **5**, 194 (1968).
[7]C. H. Griffiths and H. K. Eastwood, J. Appl. Phys. **45**, 2201 (1974).
[8]K. D. Rogers, J. A. Coath, and M. C. Lovell, J. Appl. Phys. **70**, 1412 (1991).
[9]H. J. Schlag and W. Scherber, Thin Solid Films **366**, 28 (2000).
[10]D. Brassard, S. Fourmaux, M. Jean-Jacques, J. C. Kieffer, and M. A. El Khakani, Appl. Phys. Lett. **87**, 051910 (2005).
[11]E. E. Chain, J. Vac. Sci. Technol. A **4**, 432 (1986).
[12]C. Chen, X. Yi, J. Zhang, and X. Zhao, Infrared Phys. Technol. **42**, 87 (2001).
[13]S. B. Wang, S. B. Zhou, G. Huang, and X. J. Yi, Surf. Coat. Technol. **191**, 330 (2005).
[14]J. Li and N. Yuan, Proc. SPIE **5774**, 232 (2004); J. H. Li, N. Y. Yuan, and J. S. Xie, Appl. Surf. Sci. **243**, 437 (2005).
[15]K. van Steensel, F. van de Burg, and C. Kooy, Philips Res. Rep. **22**, 170 (1967).
[16]G. A. Nyberg and R. A. Buhrman, J. Vac. Sci. Technol. A **2**, 301 (1984).
[17]S. Koide and H. Takei, J. Phys. Soc. Jpn. **22**, 946 (1967).
[18]J. B. MacChesney, H. J. Guggenheim, and J. F. Potter, J. Electrochem. Soc. **115**, 52 (1968).
[19]H. K. Kim, H. You, R. P. Chiarello, H. L. M. Chang, T. J. Zhang, and D. J. Lam, Phys. Rev. B **47**, 12900 (1993).
[20]V. N. Andreev, M. A. Gurvitch, V. K. Klimov, I. A. Khahaev, and F. A. Chudnovskiy, Tech. Phys. Lett. **19**, 283 (1993); V. N. Andreev, F. A. Chudnovskiy, and V. K. Klimov, JETP Lett. **60**, 647 (1994).
[21]D. H. Kim and H. S. Kwok, Appl. Phys. Lett. **65**, 3188 (1994); Z. P. Wu, S. Yamamoto, A. Miyashita, Z. J. Zang, K. Narumi, and N. Naramoto, J. Phys.: Condens. Matter **10**, L765 (1998).
[22]J. Narayan and V. M. Bhosle, J. Appl. Phys. **100**, 103524 (2006).
[23]K. Nagashima, T. Yanagida, H. Tanaka, and T. Kawai, J. Appl. Phys. **100**, 063714 (2006).
[24]F. A. Chudnovskiy and G. B. Stefanovich, J. Solid State Chem. **98**, 137 (1992); G. B. Stefanovich, A. L. Pergament, A. A. Velichko, and L. A. Stefanovich, J. Phys.: Condens. Matter **16**, 4013 (2004).
[25]D. P. Partlow, S. R. Gurkovich, K. C. Radford, and L. J. Denes, J. Appl. Phys. **70**, 444 (1991); Y. Ningyi, L. Jinhua, H. L. W. Chan, and L. Chenglu, Appl. Phys. A: Mater. Sci. Process. **78**, 777 (2004); M. Pan, H. Zhong, S. Wang, J. Liu, Z. Li, X. Chen, and W. Lu, J. Cryst. Growth **265**, 121 (2004).
[26]G. A. Rozgonyi and W. J. Polito, J. Electrochem. Soc. **115**, 56 (1968); also P. J. Powell, C. N. Bergland, and W. E. Spicer, Phys. Rev. **178**, 1410 (1969).
[27]I. Balberg and S. Trokman, J. Appl. Phys. **46**, 2111 (1975).
[28]See, for example, A. A. Bugaev, B. P. Zakharchenya, and F. A. Chudnovskiy, Sov. J. Quantum Electron. **9**, 855 (1979).
[29]S.-J. Jiang, C.-B. Ye, M. S. R. Khan, and C.-G. Granqvist, Appl. Opt. **30**, 847 (1991).
[30]G. Golan, A. Axelevitch, B. Sigalov, and B. Gorenstein, Microelectron. J. **34**, 255 (2003).
[31]V. I. Andreev, A. S. Oleinik, and Yu. I. Sarov, Sov. Phys. Solid State **22**, 2163 (1980); V. G. Mokerov, A. R. Verishev, and A. S. Ignat'ev, *ibid.* **21**, 855 (1979); A. S. Oleinik, Neorg. Mater. **27**, 534 (1991); A. S. Oleinik, Zh. Tekh. Fiz. **63**, 97 (1993); S. N. Svistasheva and V. N. Kruchinin, Thin Solid Films **313–314**, 319 (1998).
[32]Y.-H. Han, I.-H. Choi, H.-K. Kang, J.-Y. Park, K.-T. Kim, H.-J. Shin, and S. Moon, Thin Solid Films **425**, 260 (2003).
[33]J. He, L. Lin, Y. Lu, T. Lu, Z. Liu, and J. Wang, Proc. SPIE **6037**, 429 (2006).
[34]M. Gurvitch, S. Luryi, A. Polyakov, and J. Brinker (unpublished).
[35]F. A. Chudnovskyi (private communication).
[36]A. S. Oleinik, Tech. Phys. **47**, 1014 2002.
[37]G. I. Petrov, V. V. Yakovlev, and J. Squier, Appl. Phys. Lett. **81**, 1023 (2002).
[38]R. Srivastava and L. L. Chase, Phys. Rev. Lett. **27**, 727 (1971).
[39]C. N. Berglund and H. J. Guggenheim, Phys. Rev. **185**, 1022 (1969).
[40]R. G. Cope and A. W. Penn, Br. J. Appl. Phys. **1**, 161 (1968); J. Duchene, J. Solid State Chem. **12**, 303 (1975).
[41]P. B. Allen, R. M. Wentzcovitch, W. W. Schulz, and P. C. Canfield, Phys. Rev. B **48**, 4359 (1993).
[42]J. B. McChesney and H. J. Guggenheim, J. Phys. Chem. Solids **30**, 225 (1969).
[43]H. Bialas, A. Dillenz, H. Downar, and P. Ziemann, Thin Solid Films **338**, 60 (1999).
[44]G. A. Rozgonyi and D. H. Hensler, J. Vac. Sci. Technol. **5**, 194 (1968).
[45]R. A. Wood, Laser Focus World **29**, 101 (1993); R. A. Wood, Semicond. Semimetals **47**, 43 (1997); D. Murphy *et al.*, Proc. SPIE **5783**, 448 (2005).
[46]B. E. Cole, R. E. Higashi, and R. A. Wood, Proc. IEEE **86**, 1679 (1998).
[47]W. Radford *et al.*, Proc. SPIE **2746**, 82 (1996).
[48]H. Jerominek, F. Picard, and D. Vincent, Opt. Eng. (Bellingham) **32**, 2092 (1993).
[49]R. T. R. Kumar, B. Karunagaran, D. Mangalaraj, S. K. Narayandass, P. Manoravi, M. Joseph, and V. Gopal, Sens. Actuators, A **107**, 62 (2003).
[50]M. Gurvitch, M. Halioua, A. Kastalsky, S. Naar, and S. Shokhor, U.S. Patent No. 5,896,005 (April 20, 1999).
[51]J. Duchene, Microelectronics **4**, 37 (1972).
[52]R. T. Kivaisi and M. Samiji, Sol. Energy Mater. Sol. Cells **57**, 141 (1999).
[53]V. A. Klimov, I. O. Timofeeva, S. D. Khanin, E. B. Shadrin, A. V. Ilinskii, and F. Silva-Andrale, Tech. Phys. **47**, 1134 (2002).
[54]Y. J. Chang *et al.*, Thin Solid Films **486**, 46 (2005).
[55]JCPDS (Joint Committee on Powder Diffraction Standards) Card No. 72-0514 (unpublished).